

DFT study on the structural and electronic properties of gallium and arsenic doped silicon nanowire

R.Reenu¹, G.Saranya Devi¹, M.Rajendran*²

¹Department of Electrical and Electronics Engineering, Kamaraj College of Engineering and Technology, Virudhunagar - 626 001, Tamilnadu, India.

²Department of chemistry, Centre for Research and Post Graduate Studies in Chemistry, N. M. S. S. Vellaichamy Nadar College, Nagamalai, Madurai- 625 019, Tamilnadu, India.

Abstract: Silicon-based active optical components are nowadays becoming reliable and interesting in order to leverage the infrastructure of silicon microelectronics technology for the fabrication of optoelectronic devices. Aim of this work is the investigation of the role played by doping with donor and acceptor impurities like Gallium and Arsenic in silicon based nanostructures, like Silicon nanowires. Doping - the intentional introduction of impurities into a material is fundamental to control the properties of bulk semiconductors, and also to engineer the electronic and optical properties of nanowires for optoelectronic applications. The study of the structural and electronic properties of simultaneous n- and p-type doped hydrogenated silicon nanowires with gallium and arsenic impurities have shown that Ga-As codoping is energetically favourable with respect to single Ga or As doping and that the two impurities tend to occupy nearest neighbours sites. Density functional theory (DFT) calculations were performed to investigate the properties of planar forms of silicon nanostructures. The structure of silicon nanowires are successfully optimized and simulated using B3LYP/LanL2DZ basis set. The electronic properties were investigated in terms of ionization potential, electron affinity and HOMO-LUMO gap of silicon nanowire. The results indicated that the bond lengths between silicon and dopant atoms are varied from the Si-Si bond. The binding energies indicated that the undoped silicon nanowire form could be considered as the most stable form of silicon nanostructures among the investigated forms. Better conductivity of the doped-Si form was confirmed by the gap energies.

Keywords: Silicon, doping, Nanostructure, Density Functional Theory (DFT), Nanosheet.

Introduction

In recent years, there has been a considerable amount of theoretical and experimental interest focused on silicon nanoclusters. Present day research has been focusing on reducing the thermal conductivity of thermoelectric materials by nanoengineering, reaching the limit where the nanostructured interfaces strongly scatter phonons but only marginally affect the charge carrier transport¹. Silicon nanowires (Si-nws) are promising candidates as efficient thermoelectric materials,²⁻⁸ due to the large density of states in confined one-dimensional systems leading to an increased power factor⁹ and a potentially very low thermal conductivity, for example, through increased phonon scattering at their surface¹⁰. In this work, we provide a simple, yet effective, way to tune the thermal conductivity of nanowires by random placement of n-type and p-type nanoparticles on Si-nw arrays and measure this surface doping effect on the thermal conductivity of the entire nanowire array. Silicon nanowires and nanotubes are promising candidates for becoming the basic modules of the next generation nanoelctronic systems^{11,12}.

It is often said that silicon is the quintessential building material for electronic devices. However, silicon is more than a building material. It is a very special material that allows us to build computers and to learn much about the electronic properties of materials, *e.g.*, these computers built with silicon can be used to solve for the electronic properties of silicon itself. To illustrate this situation, an example is given of how computational approaches can be used to understand the behavior of dopants in silicon at the nanoscale.

One-dimensional silicon nano structures silicon crystallizes in a diamond-like structure forming covalent bonds in tetragonal coordination also known as sp^3 hybridization. The formation of more stable hybridized sp^3 bonds in silicon leads to four fold coordination with four equivalent directions for growth. This gives areas on why silicon nanostructures with bulk-like core are more favorable than hollow structures. Dealing with one- dimensional nanostructures, the sp^3 hybridization favors the formation of si-nw rather than si-nt (silicon nanotube).

The applications of silicon nanocrystalline particles have become an extensive and attractive area of research due to their diverse properties. Some of the most important applications involve energy conversion in photovoltaic solar cells¹³, biomedical fluorescent imaging as biological sensors¹⁴, and their electrical response in nanoelectronics as field-effect transistors^{15,16}, logic circuits¹⁷, light-emitting diodes¹⁸ etc. The physical and chemical properties of Si nano particles can be greatly influenced by their surface chemistry, size and shape. As the size of silicon nanoparticles approaches the quantum regime, their electronic properties are substantially altered compared to a bulk material, due to the strong effect of quantum confinement¹⁹.

Owing to their potential applications in optoelectronics, the study of silicon nanowires and quantum dots is a very active field of research. Optical properties of these confined systems are known to be quite different from their bulk counterparts and even from each other. In contrast with the semiconducting nature of the bulk silicon, the metallic behavior of the columns formed by nanocrystalline silicon particles was detected²⁰. The luminescence properties of the silicon nanowires have been studied experimentally in significantly less extent^{21,22}. The electroluminescence peak with the energy 600 nm (2.07 eV) was occurred from silicon nanowires with average diameter 4 nm as a result of band-to-band electron-hole recombination.

Computational works that are studying silicon nanowires and use DFT methods usually take advantage of the periodicity of a crystalline structure in order to perform calculations about their properties. These works usually employ different techniques for extracting results about electronic properties since DFT within either the generalized gradient approximation (GGA) or local density approximation (LDA)²³ underestimates band gaps, in some cases even by a factor of two¹⁹. Despite this, DFT can predict reliably the geometries and the band structure when varying the diameter or the surface of these nanoclusters. The LDA approximation has previously been successfully used to describe the electronic structure of the silicon periodic systems^{24, 25}.

2. Computational details

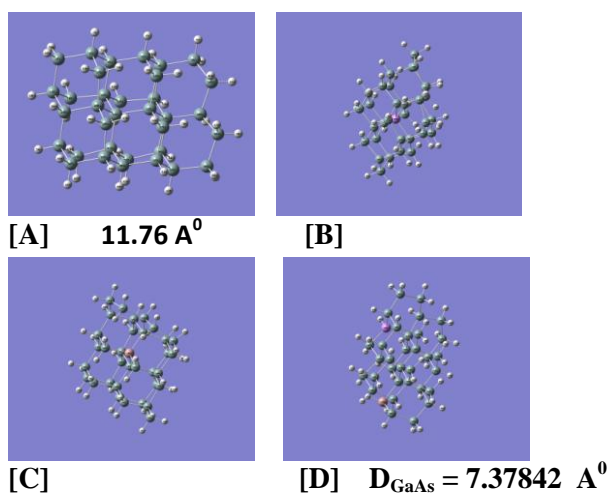


Figure -1. B3LYP/LanL2DZ optimized structure of hydrogenated Silicon nanowire in the (110) direction [A]: ($\text{Si}_{34}\text{H}_{42}$), [B]: ($\text{Si}_{33}\text{AsH}_{42}$), [C]: ($\text{Si}_{33}\text{GaH}_{42}$), [D]: ($\text{Si}_{32}\text{GaAsH}_{42}$ $D_{\text{GaAs}} = 7.3784 \text{ Å}^0$) in three layers. The brown balls are Si atoms, while the white are the surface hydrogen used to saturate the dangling bonds. The As and Ga atoms are in different colours. The relaxed impurity-impurity distance is [D]: $D_{\text{GaAs}} = 7.3784 \text{ Å}^0$

The geometries of all considered structures are fully optimized and simulated at B3LYP along with suitable LanL2DZ basis set²⁶⁻²⁸. The spin-unrestricted approach is applied to describe the geometry optimization, electronic structure of Ga and As doped nanoclusters. It is noteworthy that pure DFT methods underestimate energy gaps relative to hybrid DFT methods such as B3LYP that include Hartree–Fock exchange. Also B3LYP is the common used approach for investigations of nanostructure topics²⁹⁻³². While simulating silicon nanostructures, choosing the basis set is an important criterion. Thus, LanL2DZ basis set is a good choice to optimize silicon nanostructures³³. All calculations are performed using Gaussian 09 package³⁴. The density of states (DOS) spectrum of silicon nanostructures are drawn with the help of Gauss Sum 3.0 package³⁵.

3. Results and Discussions

In the present paper, we will present our results concerning the band gap, structure and electronic properties of n-doped, p-doped and codoped silicon nanowire (Si-nw).

3.1. Structural properties

The structural changes of the doped Si-nw have been investigated as a function of the size of the impurity position and of the number of dopant species present within the Si-nw. Figure-1 shows that B3LYP/LanL2DZ optimized structure of undoped and doped Si-nw (110) direction in three layers. The Si-nw ($\text{Si}_{34}\text{H}_{42}$) have a perfect parallel layer after optimization, however the Gallium and Arsenic doped Si-nw structure shows that in the place of impurity there is a change in bond length than the undoped one. The properties of the Si-nw were studied by substituting the Ga or As in the same place of the Si-nw. But in the codoped Si-nw Ga and As are placed in two separate places at a distance of $D_{\text{GaAs}} = 7.3784 \text{ \AA}$, 6.9947 \AA and 4.0642 \AA . Comparing the bond lengths of doped Si-nw with undoped one, it is clear that some significant relaxation occurs around the impurities. In all the cases, the local structure has C1 symmetry, with two shorter and two longer Si – Si bonds with respect to the two surfaces. The amount of relaxation around the impurity is directly related to impurity valence and their size. The amount of bond length variation is found for the pentavalent atom As, (2.4678, 2.4678, 3.1163, and 2.4861 \AA) and a trivalent Ga, (2.5451, 2.5451, 2.4399 and 2.4509 \AA) with respect to undoped silicon 2.5451, 2.4399, 2.4509 and 2.5451 \AA (Figure-2)³⁶. Besides, it is interesting to note that in the codoped case, the differences among the impurity-Si bond lengths are not much relaxed. The impurity–impurity distance in the codoped nanowire $D_{\text{GaAs}} = 7.3784 \text{ \AA}$, 6.9947 \AA and 4.0642 \AA were studied. We have calculated the Ga-As distance after a geometry relaxation. The distance between the Ga and As codoped Si-nw are studied in the nanostructure, their property were tabulated. We note that when the impurity-impurity distance of 7.3784 \AA , 6.9947 \AA and 4.0642 \AA cases, the formation energy linearly increases with decrease in Gallium and Arsenic codoped distances (Table – 2)³⁷. This fact demonstrates that a stronger interaction between the impurities, so that codoping becomes easier.

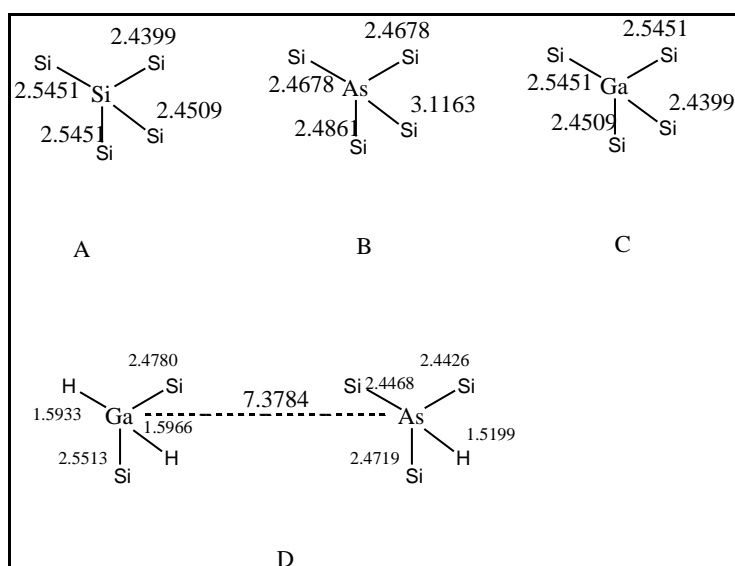


Figure - 2. Bond distances in \AA [A]: ($\text{Si}_{34}\text{H}_{42}$), [B]: ($\text{Si}_{33}\text{AsH}_{42}$), [C]: ($\text{Si}_{33}\text{GaH}_{42}$), [D]: ($\text{Si}_{32}\text{GaAsH}_{42}$ $D_{\text{GaAs}} = 7.3784 \text{ \AA}$) in three layer silicon nanowire.

3.2. Electronic properties

The role of individual dopant and codopant electronic properties of Si-nw were discussed here. When compared with the bulk system, the insertion of impurities tends to modify the electronic structure. The property of the Si semiconductor may be properly controlled by dopant size and their valence; it is possible to modulate both the electronic structure and some optical features. In the single-doped cases, the presence of either donor or acceptor states can considerably lower the energy gap of the undoped Si-nw. The bandgap of codoped Si-nw ($\text{Si}_{32}\text{GaAsH}_{42}$) was in between the individual dopant band gaps. Band gap of As doped Si-nw and Ga doped Si-nw and Codoped Si-nw ($\text{Si}_{32}\text{GaAsH}_{42}$ $D_{\text{GaAs}} = 7.3784 \text{ \AA}^0$) was 2.8319 eV, 5.2312 eV and 3.1051 eV respectively.

In $\text{Si}_{33}\text{AsH}_{42}$, the defect level is located just 0.1648 eV below the conduction band, so that the energy gap is only 0.1648 eV. Similarly for $\text{Si}_{33}\text{GaH}_{42}$, the defect level is located just 0.3271 eV above the valance band. The electronic properties of As and Ga codoped Si-nw are qualitatively different from those of either As or Ga single doped Si-nw. Now the system is a semiconductor, and the presence of both impurities leads to a HOMO – LUMO energy gap strongly lowered with respect to that of the corresponding undoped nanowires³⁸. The possibility of modulating the electronic properties of the codoped Si-nw is also evident, if we keep the distance between the impurities.

The dipole moments of undoped, As doped, Ga doped, GaAs codoped $D_{\text{GaAs}} = 7.3784 \text{ \AA}^0$, 6.9947 \AA^0 and 4.0642 \AA^0 Si-nw are calculated to be 0.1007, 1.7648, 0.8134, 14.2455, 14.0869 and 6.4597 Debye respectively. This infers that charge distributions are uniform for individual dopant. In contrast GaAs codoped Si-nw have high value of dipole moments. It reveals that the charge distributions are not uniform in the GaAs codoped Si-nw. In codoped Si-nw the dipole moment value variation was depends on distance between two impurities, as the distance decreases the dipole moment value also decreases. It implies that interaction between the two impurity increases with decrease in distance, hence charge localization decreases with lowering the distances (Table 2).

In figure - 3 only the levels corresponding to the HOMO, LUMO, HOMO-1, and LUMO+1, states are shown. The presence of donor or acceptor states lowers the energy gap (E_g). For single-doped Si-nw the HOMO level contains only one electron and is localized with As or Ga impurity as revealed by HOMO and LUMO (figure – 4). The electronic properties of As and Ga codoped Si-nw are qualitatively and quantitatively different from those of either As or Ga single doped Si-nw. E_g is reduced from 5.5562 eV of pure Si-nw to 3.1052 eV of the $\text{Si}_{32}\text{AsGaH}_{42}$ ($D_{\text{GaAs}} = 7.37842 \text{ \AA}^0$) nanowire. The HOMO and LUMO states progressively localize on the impurities on going from the pure to the codoped Si-nw, where HOMO is localized on Ga and LUMO on As impurity³⁹.

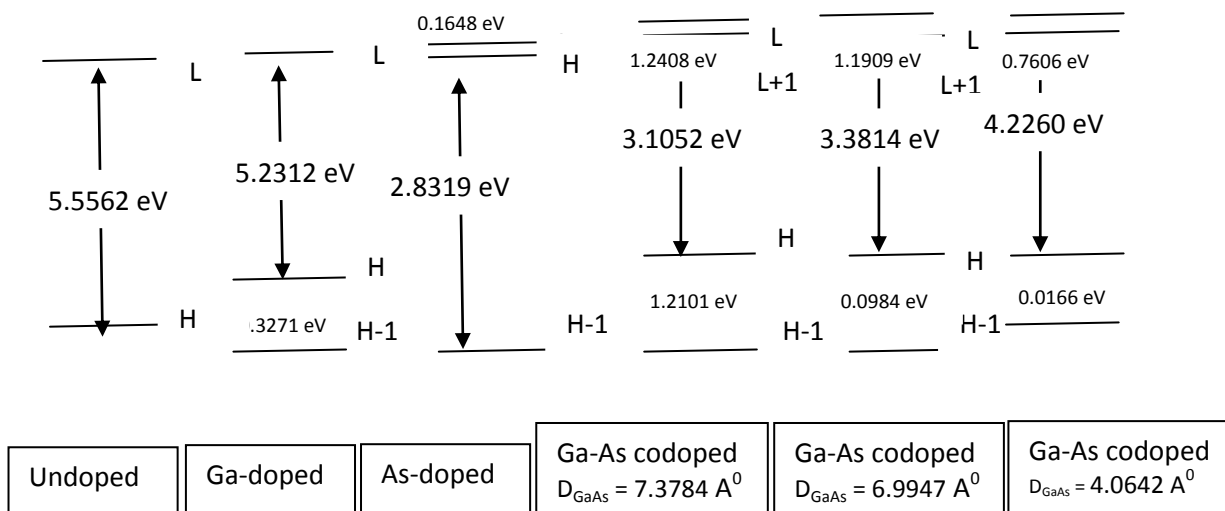


Figure - 3. Calculated energy levels for undoped ($\text{Si}_{34}\text{H}_{42}$), Ga-doped ($\text{Si}_{33}\text{GaH}_{42}$), As-doped ($\text{Si}_{33}\text{AsH}_{42}$), Ga-As-codoped ($\text{Si}_{32}\text{GaAsH}_{42}$ $D_{\text{GaAs}} = 7.3784 \text{ \AA}^0$), ($\text{Si}_{32}\text{GaAsH}_{42}$ $D_{\text{GaAs}} = 6.9947 \text{ \AA}^0$) and ($\text{Si}_{32}\text{GaAsH}_{42}$ $D_{\text{GaAs}} = 4.0642 \text{ \AA}^0$) in three layers silicon nanowire.

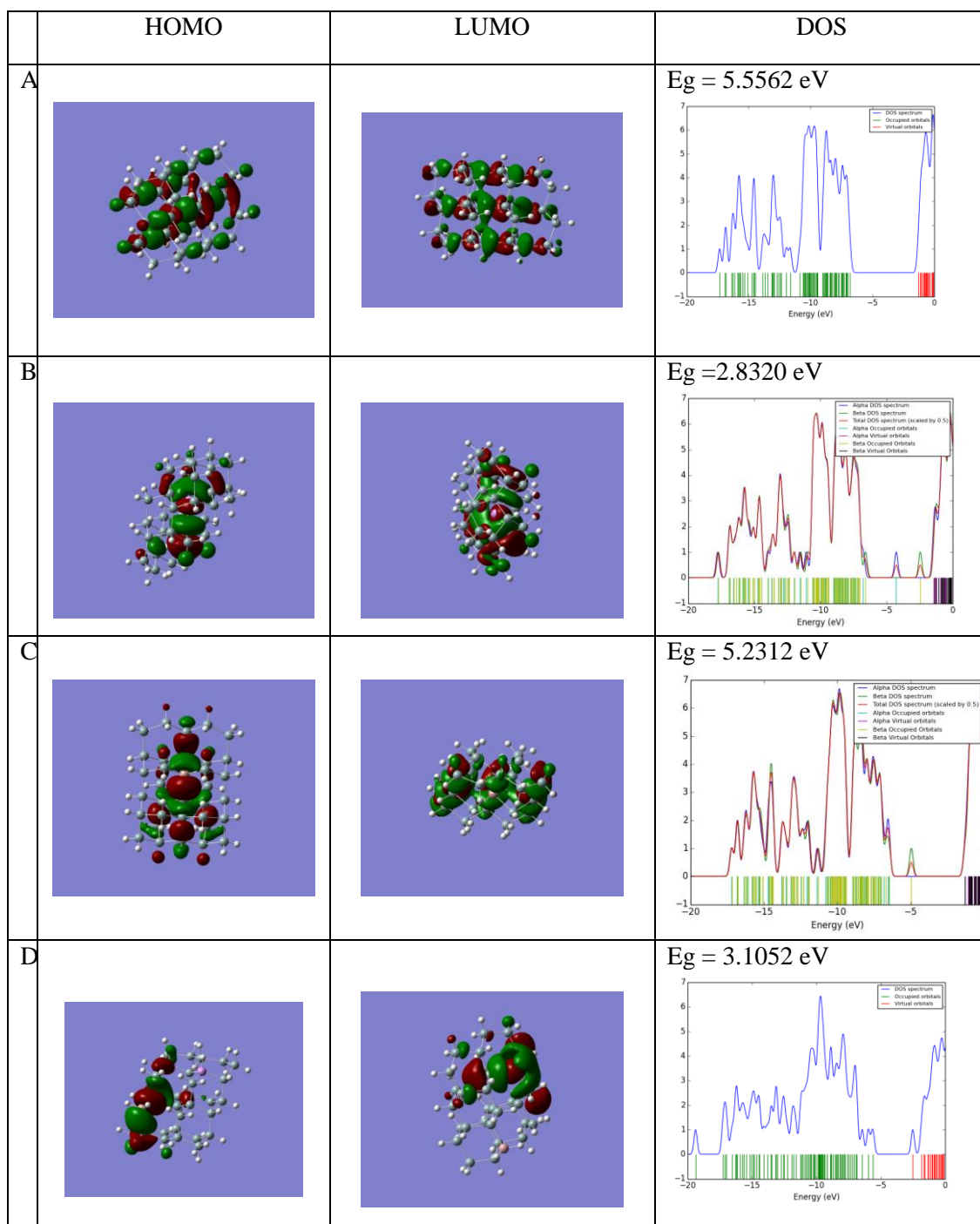


Figure - 4. HOMO, LUMO and DOS of [A]: ($\text{Si}_{34}\text{H}_{42}$), [B]: ($\text{Si}_{33}\text{AsH}_{42}$), [C]: ($\text{Si}_{33}\text{GaH}_{42}$), [D]: ($\text{Si}_{32}\text{GaAsH}_{42}$ $D_{\text{GaAs}} = 7.3784 \text{ \AA}^0$) in three layers silicon nanowire.

The insertion of impurities strongly modifies the electronic structure, in particular it is interesting to see, looking at figure-3, how the simultaneous insertion of both As and Ga changes the electronic properties of Si-nw, with respect to the single doped cases. Now the system is a semiconductor, and the presence of both impurities leads to a HOMO level that contains two electrons and to a HOMO-LUMO energy gap strongly lowered with respect to that of the corresponding undoped nanowire. Figure 3 shows that the energy levels of $\text{Si}_{34}\text{H}_{42}$ and $\text{Si}_{32}\text{GaAsH}_{42}$, with the impurities located at two different distances. The impurities are placed at a distance $D_{\text{GaAs}} = 7.3784 \text{ \AA}^0$, 6.99472 \AA^0 and 4.0642 \AA^0 , for this particular nanowire. From the figure-3, it is evident that when impurities are at the larger distance, E_g is strongly reduced with respect to the corresponding lower distanced Ga-As Si-nw. On the contrary, when the impurities are close to each other, E_g enlarges ($E_g = 4.2260 \text{ eV}$). The reason for the E_g variation with respect to distance may be when impurities are brought closer, the Coulomb interaction becomes stronger so that energy gap becomes larger. We observe that E_g decreases with the increase of the impurity distance. It is possible to tune E_g as a function of the impurity-impurity

distance⁴⁰. The possibility of modulating the electronic properties of the codoped Si-nw is also evident if we keep the distance between the impurities constant and look at the dependence of the energy gap on the Si-nw.

Table-1 Undoped and doped optimized Silicon nanowire (Si₃₄H₄₂) properties

Properties	Undoped Si (Si ₃₄ H ₄₂)	Ga doped Si (Si ₃₃ GaH ₄₂)	As doped Si (Si ₃₃ AsH ₄₂)
Basis set	B3LYP/LanL2DZ	UB3LYP/LanL2dz	UB3LYP/LanL2dz
Enthalpy of formation (hartree)	-157.5117265	-155.6410807	-159.6925199
Symmetry	C1	C1	C1
Dipole moment (Debye)	0.1007	0.8134	1.7648
Spin	Singlet	Doublet	Doublet
HOMO (eV)	-6.830212	-6.5031237 eV	-4.2709234
LUMO (eV)	-1.27406 eV	-1.271888 eV	-1.438970
Ionization Potential (I) (eV)	6.830212	6.5031237	4.2709234
Electron Affinity (A) (eV)	1.27406 eV	1.271888	1.438970
Energy gap (ΔE)(eV)	5.55615	5.2312357	2.8319534
Chemical Hardness η (eV)	2.778075	2.61561785	1.4159767
Chemical Potential μ (eV)	-4.045213	-3.88750585	-2.8549467
Electronegativity χ (eV)	4.045213	3.88750585	2.8549467

Table-2: The properties of the codoped Silicon nanowire (Si₃₂ GaAsH₄₂) at various distances

Properties	GaAs doped Si (Si ₃₂ GaAsH ₄₂) $D_{\text{GaAs}} = 7.3784\text{\AA}^0$	GaAs doped Si (Si ₃₂ GaAsH ₄₂) $D_{\text{GaAs}} = 6.9947\text{\AA}^0$	GaAs doped Si (Si ₃₂ GaAsH ₄₂) $D_{\text{GaAs}} = 4.0642\text{\AA}^0$
Basis set	RB3LYP/LanL2dz	RB3LYP/LanL2dz	RB3LYP/LanL2dz
Enthalpy of formation (hartree)	-157.86772428	-157.89087083	-157.91818
Symmetry	C1	C1	C1
Dipole moment (Debye)	14.2455	14.0869	6.4597
Spin	singlet	singlet	Singlet
HOMO (eV)	-5.620094	-5.846226	-6.3594 eV
LUMO (eV)	-2.514933 eV	-2.464862 eV	-2.1334 eV
Ionization Potential (I) (eV)	5.620094	5.846226	6.3594
Electron Affinity (A) (eV)	2.514933	2.464862	2.1334
Energy gap (ΔE)(eV)	3.105161	3.381364	4.2260
Chemical Hardness η (eV)	1.5525805	1.690682	2.1130
Chemical Potential μ (eV)	-4.0675135	-4.155544	-4.2464
Electronegativity χ (eV)	4.0675135	4.155544	4.2464

In the single-doped cases we have already shown that the presence of donor or acceptor states can a considerably lower the energy gap of the undoped Si-nw^{41,42}. In the case of a single-doped Si-nw the gap is now defined as the energy difference between the impurity level that contains only one electron in HOMO and LUMO level. For the two single-doped Si-nw the energy gap is reduced to 0.1649 eV for As-single doped and only to 0.3271 eV for Ga-single doped Si-nw due to the presence of new impurity states located near the corresponding conductance and valence band edges (0.3271 eV above the previous valence band and 0.16491 eV below the previous conduction band respectively). For the codoped case ($D_{\text{GaAs}} = 7.3784 \text{ \AA}^0$), instead the presence of both the two kind of impurities lead to a HOMO level that contains two electrons and to a semiconductor systems, where HOMO-LUMO energy gap is severely lowered with respect to that of the corresponding undoped system (3.1052 eV $D_{\text{GaAs}} = 7.3784 \text{ \AA}^0$ with respect to 5.5562 eV) (Table-1). The structural stability of Si-nw can also be discussed in terms of chemical hardness and chemical potential. Chemical potential and chemical hardness can be calculated using the equation $\mu = -(\text{IP} + \text{EA})/2$ and $\eta = (\text{IP} - \text{EA})/2$ respectively as shown in Table-1 & 2.

3.3. Ga-As-Codoped silicon nanowires properties

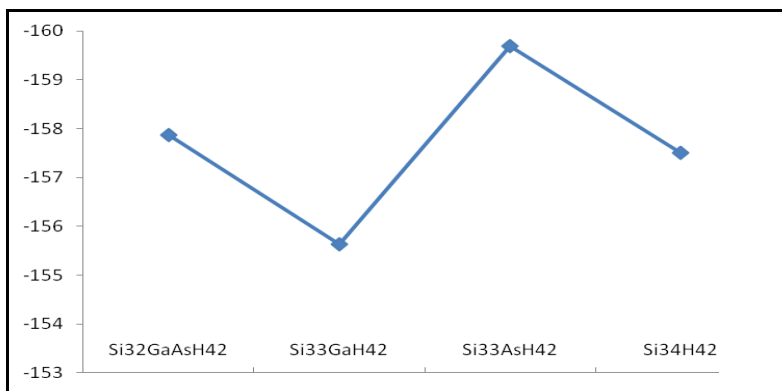


Figure - 5. Silicon nanowire formation energy (hartree) as a function of single-doped and codoped $D_{\text{GaAs}} = 7.3784 \text{ \AA}^0$ in (110) direction

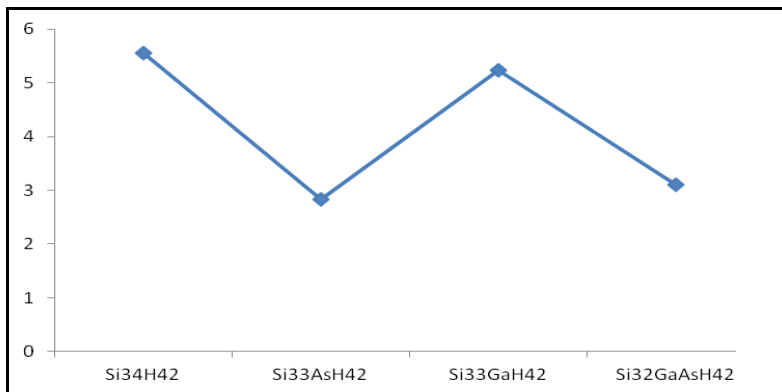


Figure - 6. Silicon nanowire of single-doped and codoped $D_{\text{GaAs}} = 7.3784 \text{ \AA}^0$ as a function of the calculated energy bandgap (eV)

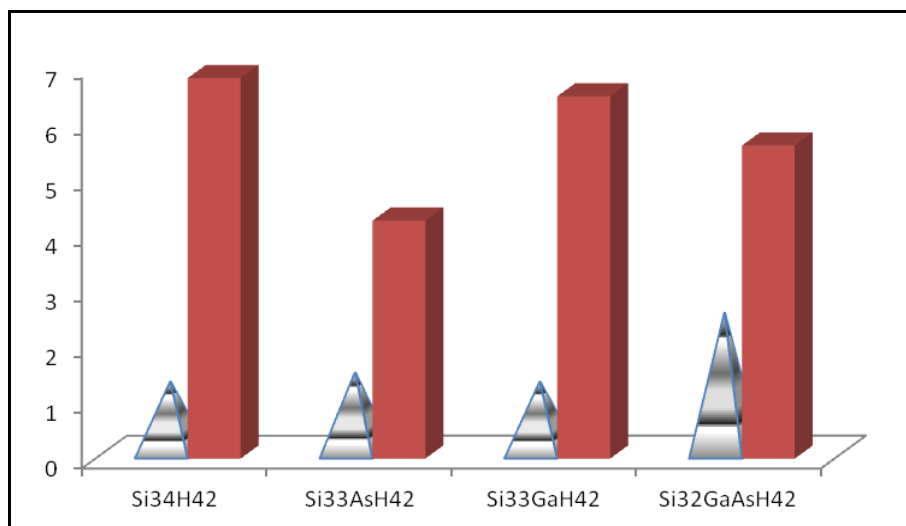


Figure - 7. Electron affinity (eV) (Pyramid) and Ionization Potential (eV) (Red Box) of silicon nanowires.

In the case of Ga and As codoped Si-nw the quantum confinement effect on the structural, electronic properties of acceptor and donor states are explored here. Si-nw has increasing interest since it has been shown that they are together with carbon nanotubes, potential candidates to build future nanoelectronic and nanophotonic devices⁴³⁻⁴⁵. In fact they offer the big advantage to be compatible with the existing silicon-based microelectronics. The possibility to tailor their electronic properties by changing thickness, orientation, surface morphology and doping is another important point⁴⁶⁻⁴⁷. The experimental study of properties like structure, surface morphology and electronic properties are very difficult task. Theoretical based a reliable ab initio DFT investigations are helpful to grow Si-nw suitable for a particular applications. Several ab initio studies on Si-nw are present in the literature. They are mainly concentrated on H-passivated Si-nw and demonstrate the dependence of the energy gap from the wire diameter and from the surface morphology⁴⁸⁻⁵³.

In the present investigation we aim to resume the main outcome of this work and illustrate specific results only for one codoped H-passivated Si-nw (with a linear cross-section $l = 1.176$ nm, grown in the (110) direction, done of 34 silicon and 42 H atoms in the unit cell). The obtained results are summarized here. From the study on Si nanoclusters, we can expect that electronic and optical properties are influenced by the doping and in fact it is evident from figure-4. The atomic structure and impurity positions of Ga-As codoped wire were shown in Fig 1(D). Looking at the structural properties, it is interesting to note that in the codoped case the differences among the four, impurity-Si bond lengths are closer with respect to the single doped case. Thus if carriers in the Si-nw are perfectly compensated by simultaneous doping with n- and p-type impurities, an almost tetrahedral configuration is recovered in which the four, impurity-Si bonds practically the same. Figure - 5 shows that the simultaneous (Ga-As) doping, the formation energy is in between the individual dopant energy cases, the codoped Si-nw is also stable one. The codoped Ga-As Si-nw formation energy is negative, indicating that formation of Ga-As codoped Si-nw is more favoured. Si-nw can be more easily simultaneously doped than single doped; this is a consequence of a charge transfer which entails a minor structural deformation. Figure-3 shows that the electronic structure varies when the two impurities are located at a different distance ($D_{\text{GaAs}} = 7.3784 \text{ \AA}^0$) with respect to $D_{\text{Si-Si}} = 2.4399 \text{ \AA}^0$) the energy gap shrinks from 5.5562 eV to 3.1052 eV. It is clear that, in principle, it is possible to tune E_g as a function of the impurity-impurity distance. The energy gap of 3.1052 eV for $\text{Si}_{32}\text{GaAsH}_{42}$ $D_{\text{GaAs}} = 7.37842 \text{ \AA}^0$, 3.3814 eV for $\text{Si}_{32}\text{GaAsH}_{42}$ $D_{\text{GaAs}} = 6.9947 \text{ \AA}^0$ and 4.2260 eV for $\text{Si}_{32}\text{GaAsH}_{42}$ $D_{\text{GaAs}} = 4.0642 \text{ \AA}^0$. The distance between the impurity-impurity levels will modulate the property of Si-nw. Figure - 6 shows that the energy gap of the codoped (Ga-As) is the average of the individual dopant Ga and As energy gaps. The electronic properties of Si-nw can also be analysed by electron affinity (EA) and ionization potential (IP). Figure- 7 shows that the EA and IP of Si-nw, the IP values are calculated for all Si-nw and the value for the n-doped and p-doped Si-nw lower than the undoped one. The Ga-As codoped Si-nw IP value was in between the two individual dopants Si-nw. The EA play a vital role in chemical sensors and plasma physics. The observed EA values are increasing from the undoped to As doped, Ga doped and GaAs codoped within the range of 1.27-2.51 eV. It implies that the moderately small amounts of energies are released due to addition of electron in Si-nw.

Conclusion

The realistic structures of undoped, Ga and As doped Si-nw are successfully simulated using B3LYP/LanL2DZ basis set. The structural stability of Si-nw was studied using calculated energy, chemical potential and hardness. Upon passivation of dangling bonds with hydrogen atom, the dangling-bond surface states disappear and the metallic nanowire becomes semiconductor with sizable band gap. It has been known that due to confinement effects band gap normally increases with decreasing diameter in the range of 1-2 nm but is stabilized at a constant value for large diameter. Our results demonstrate that codoped nanostructures present valence and conduction band-edge states which are localized on the two impurities respectively and the energy band-gap are always lower in energy with respect to that of pure undoped Si-nw. We have shown that in n-doped and p-doped Si-nw, the structural deformation around the impurity depends on both the impurity valence and impurity position. The structural and electronic properties of Si-nw codoped with Ga and As impurities have been studied. Moreover, the study of the electronic properties shows that for the simultaneously Ga- and As doped Si-nw both HOMO and LUMO are localized around the impurity sites this strongly lowering the E_g with respect to that of the pure Si-nw. This fact allows electronic transitions between donor and acceptor states, making it possible to engineers the electronic properties.

References

1. Sansoz F. Surface Faceting Dependence of Thermal Transport in Silicon Nanowires. *Nano Lett.*, 2011, 11; 5378-5382.
2. Dresselhaus MS, Chen G, Tang MY, Yang RG, Lee H, Wang DZ, Ren ZF, Fleurial JP, Gogna P. New Directions for Low-Dimensional Thermoelectric Materials. *Adv Mater*, 2007, 19; 1043-1053.
3. Hochbaum AI, Yang P. Semiconductor Nanowires for Energy Conversion. *Chem Rev.*, 2010, 110; 527-546.
4. Boukai AI, Bunimovich Y, Tahir-Kheli J, Yu JK, Goddard WA III, Heath JR. Silicon nanowires as efficient thermoelectric materials. *Nature*, 2008, 451; 168-171.
5. Hochbaum AI, Chen R, Delgado RD, Liang W, Garnett EC, Najarian M, Majumdar A, Yang P. Enhanced thermoelectric performance of rough silicon nanowires. *Nature*, 2008, 451; 163-167.
6. Li D, Wu Y, Kim P, Shi L, Yang P, Majumdar A. Thermal conductivity of Si/SiGe superlattice nanowires. *Appl Phys Lett.*, 2003, 83; 3186-3188.
7. Zou J, Balandin AA. Phonon heat conduction in a semiconductor nanowire. *J Appl Phys.*, 2001, 89; 2932-2938.
8. Pokatilov EP, Nika DL, Balandin AA. Acoustic-phonon propagation in rectangular semiconductor nanowires with elastically dissimilar barriers. *Phys Rev B*, 2005, 72; 113311.
9. Hicks LD, Dresselhaus MS. Thermoelectric figure of merit of a one-dimensional conductor. *Phys Rev B*, 1993, 47; 16631(R).
10. Donadio D, Galli G. Atomistic Simulations of Heat Transport in Silicon Nanowires. *Phys Rev Lett.*, 2009, 102; 195901.
11. Wu Y, Cui Y, Huynh L, Barrelet CJ, Bell DC, Lieber CM. Controlled Growth and Structures of Molecular-Scale Silicon Nanowires. *Nano Lett.*, 2004, 4; 433-436.
12. Rurali R, Lorente N. Metallic and Semimetallic Silicon $\langle 100 \rangle$ Nanowires. *Phys Rev Lett.*, 2005, 94; 026805.
13. Stupca M, Alsalhi M, Al Saud T, Almuhanha A, Nayfeh MH. Enhancement of polycrystalline silicon solar cells using ultrathin films of silicon nanoparticle. *Appl Phys Lett.*, 2007, 91; 063107.
14. Cui Y, Wei Q, Park H, Lieber CM. Nanowire nanosensors for highly sensitive and selective detection of biological and chemical species. *Science*, 2001, 293; 1289-1292.
15. Cui Y, Lieber CM. Functional nanoscale electronic devices assembled using silicon nanowire building block. *Science*, 2001, 291; 851-853.
16. Koo S-M, Li Q, Edelstein MD, Richter CA, Vogel EM. Enhanced channel modulation in dual-gated silicon nanowire transistors. *Nano Lett.*, 2005, 5; 2519-2523.
17. Huang MH, Mao S, Feick H, Yan H, Wu Y, Kind H, Weber E, Russo R, Yang P. Room-temperature ultraviolet nanowire nanolasers. *Science*, 2001, 292; 1897-1899.
18. Huang Y, Duan X, Cui Y, Lathon LJ, Kim K-H, Lieber CM. Logic gates and computation from assembled nanowire building blocks. *Science*, 2001, 294; 1313-1317.
19. Zhao X, Wei CM, Yang L, Chou MY. Quantum confinement and electronic properties of silicon nanowires. *Phys Rev Lett.*, 2004, 92; 236805.

20. Chen Q., Li X.-J, Zhang S, Zhu J, Zhou G, Ruan KQ, Zhang Y. Silicon quantum dot super lattice and metallic conducting behaviour in porous silicon. *J Phys Condens Matter*, 1997, 9; L569.
21. Pan H, Chen WZ, Lim SH, Poh CK, Wu XB, Feng YuP, Ji W, Lin JY. Photoluminescence and optical limiting properties of silicon nanowires. *J Nanosci & Nanotechnol.* 2005, 5; 733-737.
22. Huo J, Solanki R, Freeouf JL, Carruthers JR. Electroluminescence from silicon nanowires. *Nanotechnol.*, 2004, 15; 1848-1850.
23. Jensen F: *Introduction to Computational Chemistry* (New York: Wiley) 1999.
24. Zhao Y, Kim Y.-H, Du M.-H, Zhang SB. First-Principles Prediction of Icosahedral Quantum Dots for Tetravalent Semiconductors. *Phys Rev Lett.* 2004, 93; 015502.
25. Ruruli R, Lorente N. Metallic and Semimetallic Silicon <100> Nanowires. *Phys Rev Lett.* 2005, 94; 026805.
26. Chandiramouli R. A DFT study on the structural and electronic properties of Barium Sulfide nanoclusters, *Res J Chem Environ.*, 2013, 17; 64-73.
27. Nagarajan V, Chandiramouli R. Effect on the structural stability and electronic properties of impurity substituted sodium selenide nanostructures—A quantum chemical study. *Int J Chem Tech Res.*, 2014, 6; 2240-2246.
28. Nagarajan V, Chandiramouli R. Investigation on the structural stability and electronic properties of InSb nanostructures – A DFT approach. *Alexandria Engineering Journal*, 2014, 53; 437–444.
29. Shakerzadeh E. A theoretical study on the influence of carbon and silicon doping on the structural and electronic properties of (BeO)₁₂ nanocluster. *J Inorg Organomet Polym.*, 2014, 24; 694-705.
30. Shakerzadeh E. A theoretical study on pristine and doped germanium carbide nanoclusters. *J Mater Sci: Mater Electron.*, 2014, 25; 4193-4199.
31. Ni MY, Zeng Z, Ju X. First-principles study of metal atom adsorption on the boron-doped carbon nanotubes. *Microelectron J*, 2009, 40; 863-866.
32. Ahmadi A, Beheshtian J, Hadipour NL. Interaction of NH₃ with aluminum nitride nanotube: Electrostatic vs. covalent. *Physica E*, 2011, 43; 1717-1719.
33. Srinivasaraghavan R, Chandiramouli R, Jeyaprakash BG, Seshadri S. Quantum chemical studies on CdO nanoclusters stability. *Spectrochim. Acta, Part A*, 2013, 102; 242-249.
34. Frisch MJ, Trucks GW, Schlegel HB, Scuseria GE, Robb MA, Cheeseman JR, Zakrzewski VG, Montgomery Jr. JA, Stratmann RE, Burant JC, Dapprich S, Millam JM, Daniels AD, Kudin KN, Strain MC, Farkas O, Tomasi J, Barone V, Cossi M, Cammi R, Mennucci B, Pomelli C, Adamo C, Clifford S, Ochterski J, Petersson GA, Ayala PY, Cui Q, Morokuma K, Malick DK, Rabuck AD, Raghavachari K, Foresman JB, Cioslowski J, Ortiz JV, Baboul AG, Stefanov BB, Liu G, Liashenko A, Piskorz P, Komaromi I, Gomperts R, Martin RL, Fox DJ, Keith T, Al-Laham MA, Peng CY, Nanayakkara A, Gonzalez C, Challacombe M, Gill PMW, Johnson B, Chen W, Wong MW, Andres JL, Gonzalez C, Head- Gordon M, Replogle ES, J.A. Pople JA: *Gaussian 09 Inc.*, Pittsburgh, 2009.
35. O'boyle NM, Tenderholt AL, Langner KM, CClib. A library for package-independent computational chemistry algorithms. *J Comput Chem.*, 2007, 29; 839-845.
36. Iori F, Degoli E, Luppi E, Magri R, Marri IV, Cantele G, Ninno D, Trani F, Pulci O, Ossicini S. Engineering silicon nanocrystals: Theoretical study of the effect of codoping with boron and phosphorus. *Physical Review B*, 2007, 76; 085302.
37. Jingbo L, Linwang W, Suhuai W: Electronic structure of semiconductor nanocrystals. *Chinese Journal of semiconductors.*, 2006, 27; 191-196.
38. Fujii M, Toshikiyo K, Takase Y, Yamaguchi Y, Hyashi S. Below bulk-band-gap photoluminescence at room temperature from heavily P-and B-doped Si nanocrystals. *J Appl Phys.*, 2003, 94; 1990.
39. Ossicini S, Bisi O, Degoli E, Marri I, Iori F, Luppi E, Magri R, Poli R, Cantele G, Ninno D, Trani F, Marsili M, Pulci O, Olevano V, Gatti M, Gaal-Nagy K, Incze A, Onida G. First-principles study of silicon nanocrystals: Structural and electronic properties, absorption, emission and doping. *J Nanosc. Nanotechnol.* 2007, X; 1-14.
40. Ossicini S, Degoli E, Iori F, Luppi E, Magri R, Cntele G, Trani F, Ninno D. *Appl Phys Lett.*, 2005, 87; 173120.
41. Cantele G, Degoli E, Luppi E, Magri R, Ninno D, Iadonisi G, Ossicini S. Simultaneously B-and P-doped silicon nanoclusters: Formation energies and electronic properties. *Phys Rev.*, B 2005, 72; 113303.
42. Ossicini S, Degoli E, Iori F, Luppi E, Magri R, Cantele G, Trani F, Ninno D. Simultaneously B- and P-doped silicon nanoclusters: Formation energies and electronic properties. *Appl Phys Lett.*, 2005, 87; 173120.

43. Cui Y, Zhong Z, Wang D, Wang W, Lieber C. High Performance Silicon Nanowire Field Effect Transistors. *Nano Lett.*, 2003, 3; 149-152.
44. Cui Y, Lieber CM. Functional Nanoscale Electronic Devices Assembled using Silicon Nanowire Building Blocks. *Science.*, 2001, 291; 851-853.
45. Cui Y, Wei Q, Park H, Lieber C: Nanowire Nanosensors for Highly Sensitive and Selective Detection of Biological and Chemical Species. *Science.*, 2001, 293; 1289-1292.
46. Cui Y, Duan X, Lieber C: Doping and Electrical Transport in Silicon Nanowires. *J Phys Chem B.*, 2000, 104; 5213-5216.
47. Ma D, Lee CSS, Lee ST: Scanning tunneling microscopic study of boron-doped silicon nanowires. *Appl Phys Lett.*, 2001, 79; 2468-2470.
48. Buda F, Kohanoff J, Parrinello M. Optical properties of porous silicon. A first-principles study. *Phys Rev Lett.*, 1992, 69; 01272.
49. Read AJ, Needs RJ, Nash KJ, Canham LT, Calcott PDJ, Qteish A. First-principles calculations of the electronic properties of silicon quantum wires. *Phys Rev Lett.*, 1992, 69; 1232.
50. Kagimura R, Nunes RW, Chacham H. Structures of Si and Ge Nanowires in the Subnanometer Range. *Phys. Rev. Lett.*, 2005, 95; 115502.
51. Rurali R, Lorente N: Metallic and Semimetallic Silicon $\langle 100 \rangle$ Nanowires. *Phys Rev Lett.*, 2005, 94; 026805.
52. Zhao X, Wei CM, Yang L, Chou MY: Quantum Confinement and Electronic Properties of Silicon Nanowires. *Phys Rev Lett.*, 2004, 92; 236805.
53. Bruno M, Palumbo M, Marini A, Del Sole R, Ossicini S. From Si Nanowires to Porous Silicon: The Role of Excitonic Effects. *Phys Rev Lett.*, 2007, 98; 036807.

International Journal of ChemTech Research

[www.sphinxesai.com]

Publish your paper in Elsevier Ranked, SCOPUS Indexed Journal.

[1] RANKING:

has been ranked **NO. 1**. Journal from India (subject: **Chemical Engineering**) from India at **International platform**, by **SCOPUS**- scimagojr.

It has topped in total number of CITES AND CITABLE DOCUMENTS.

Find more by clicking on **Elsevier- SCOPUS SITE....AS BELOW.....**

<http://www.scimagojr.com/journalrank.php?area=1500&category=1501&country=IN&year=2011&or>

[der=cd&min=0&min_type=cd](http://www.scimagojr.com/journalrank.php?area=1500&category=1501&country=IN&year=2011&or)

Please log on to - www.sphinxesai.com

[2] Indexing and Abstracting.

International Journal of ChemTech Research is selected by -

CABI, CAS(USA), **SCOPUS**, MAPA (India), ISA(India),DOAJ(USA),Index Copernicus, Embase

database, EVISA, DATA BASE(Europe), Birmingham Public Library, Birmingham, Alabama, RGATE

Databases/organizations for Indexing and Abstracting.

It is also in process for inclusion in various other databases/libraries.

[3] Editorial across the world. [4] Authors across the world:

For paper search, use of References, Cites, use of contents etc in- International Journal of ChemTech Research,

Please log on to - www.sphinxesai.com
